CHALMERS

Publication 01/05

An experimental investigation of the flow in the spiral casing and distributor of the Hölleforsen Kaplan turbine model

Håkan Nilsson, Urban Andersson and Sebastian Videhult

Department of Thermo and Fluid Dynamics
CHALMERS UNIVERSITY OF TECHNOLOGY
Göteborg, Sweden, September 2001

An experimental investigation of the flow in the spiral casing and distributor of the Hölleforsen Kaplan turbine model

H. Nilsson[1], U. Andersson[2] and S. Videhult[3]

Abstract

This work experimentally studies the flow in the spiral casing and distributor of the Hölleforsen Kaplan water turbine model. The measurements are an extension of the measurements for the *Turbine 99* and *Turbine 99 - II* workshops. The velocity distribution in the spiral casing and distributor is measured with the LDV (Laser Doppler Velocimetry) technique. The work is a collaboration between three projects in the Swedish water turbine program.

This paper reports the achievements of the extended measurements requested by ELFORSK, who financed the work.

1 Introduction

The Hölleforsen Kaplan model draft tube was thoroughly investigated in the *Turbine 99* workshop on draft tube flow [1, 3], in 1999. The measurements were pressure measurements along the upper and lower centerlines of the draft tube wall and LDV measurements of the velocity distribution at several locations. The LDV measurements were made in a number of cross-sections in the draft tube and along profiles close to the end of the runner cone and close to the runner blade suction side [2]. The velocity distribution measured close to the runner blade suction side was used as an inlet boundary condition for the *Turbine 99* contributions and the remainder of the measurements were used for validation of the draft tube computational results.

The *Turbine 99* measurements were made as part of one of the projects in the Swedish water turbine program, financed and supported by ELFORSK (Swedish Electrical Utilities Research and Development Company), the Swedish National Energy Administration and GE Energy (Sweden) AB. Two of the projects in the Swedish water turbine program numerically study the flow in Kaplan turbine spiral casings, distributors and runners. Taking advantage of the experience of the measurement techniques from the *Turbine 99* measurements and the availability of the Hölleforsen model, a collaboration between the projects in the Swedish water turbine program was established.

The main goal of the collaboration was to extend the previous measurements with measurements in the spiral casing and distributor. The measurements will be used for validation of ongoing computations of the flow in the distributor and for future computations in spiral casings. The collaboration also contributes to an increasing knowledge of the turbine behaviour, since a combination of measurements and computations gives a detailed and accurate picture of the flow. Runner computations that are validated against *Turbine 99* measurements and the measurements in this work may contribute to the removal of some of the uncertainties encountered during the workshop, such as the draft tube inlet radial velocity component. The extended measurements were made in conjuction with the last measurement period for the *Turbine 99 -*

[1]CHALMERS, Thermo and Fluid Dynamics, S - 412 96 Gothenburg
[2]Vattenfall Utveckling AB, S - 814 26 Älvkarleby
[3]GE Energy (Sweden) AB, P.O. Box 1005, S - 681 29 Kristinehamn

II workshop, which keeps the costs at a minimum and takes advantage of the experience gained in the workshop measurements.

2 Description of the Hölleforsen Kaplan turbine model

The Hölleforsen Kaplan turbine test rig is thoroughly described by Marchinkiewicz and Svensson [6].The Hölleforsen power plant was installed in 1949. The head of the power plant, which is situated in Indalsälven in Sweden, is $27m$ and consists of three Kaplan turbines with a runner diameter of $5.5m$, maximum power of $50MW$ and flow capacity of $230m^3/s$ per turbine. The model runner has a diameter of $D = 0.5m$, and it is possible to alter the runner blade angle, the guide vane opening, the runner speed and the test head. The measurements in this work were made at a head of $H = 4.5m$, a runner speed of $N = 595rpm$ (unit runner speed, $DN/\sqrt{H} = 140$) and a volume flow of $Q = 0.522m^3/s$ (unit flow, $Q/D^2\sqrt{H} = 0.98$). This operating condition is close to the best efficiency operating point, at 60% load.

3 Measurement specifications

The measurements presented in this work are made with the LDV (Laser Doppler Velocimetry) technique. The technique, with its limitations and error sources, is thoroughly described by Andersson [3]. A brief description of the technique is presented below.

The LDV technique is a non-intrusive method that uses the Doppler shift of reflected light from particles to determine the instantaneous velocity in a single point. The resulting Doppler frequency is proportional to the measured velocity. Calibration is thus not necessary. The main disadvantage of the LDV technique is the need of visual access. The fluid and model walls (preferably flat) must be transparent. A number of plexiglass windows have thus been installed in the Hölleforsen Kaplan model.

The LDV system is a two-component fibre-optic system from TSI Inc, with IFA 750 signal processors. With this equipment, two orthogonal velocity components may be measured at the same time. The focal length of the probe is $500mm$ and the distance between the beams is $50mm$. This configuration gives a measurement volume of an approximate length of $2.5mm$ and diameter of $124\mu m$ (mean values of the wave lengths $488.0nm$ and $514.5nm$). The water was seeded with nylon particles ($d = 4.2\mu m$, $\rho_p/\rho_w = 1.02$) that follow the flow satisfactorily. The amount of particles was adjusted to achieve an approximate data rate of 100 collected bursts per second. The total sampling time was set to $120s$ or 20000 bursts for the measurements in the spiral casing and $180s$ or 40000 bursts for the measurements in the distributor. The probe is positioned with an automatic traverse table from ISEL, which can repeat a position within $0.1mm$. The LDV measurements were made in *single measurement per burst mode*, which means that only one velocity measurement is made of each particle.

No manipulation of time series, e.g. exclusion of single readings, was done. All types of measurements contain systematic deviations, such as bias phenomena, that can be corrected with correction formulas. The time and space resolutions affect the evaluation and interpretation of the measurements. The time and space resolutions in this work are sufficient for a detailed picture of the mean velocity values and RMS values, but are not good enough for a detailed investigation of the turbulent time and space scales. The sampling time was increased in the distributor in order to find periodic behaviour originating in the runner blade passage. Due to the randomness of the velocity realisations, each period lacks data, but overlaying several

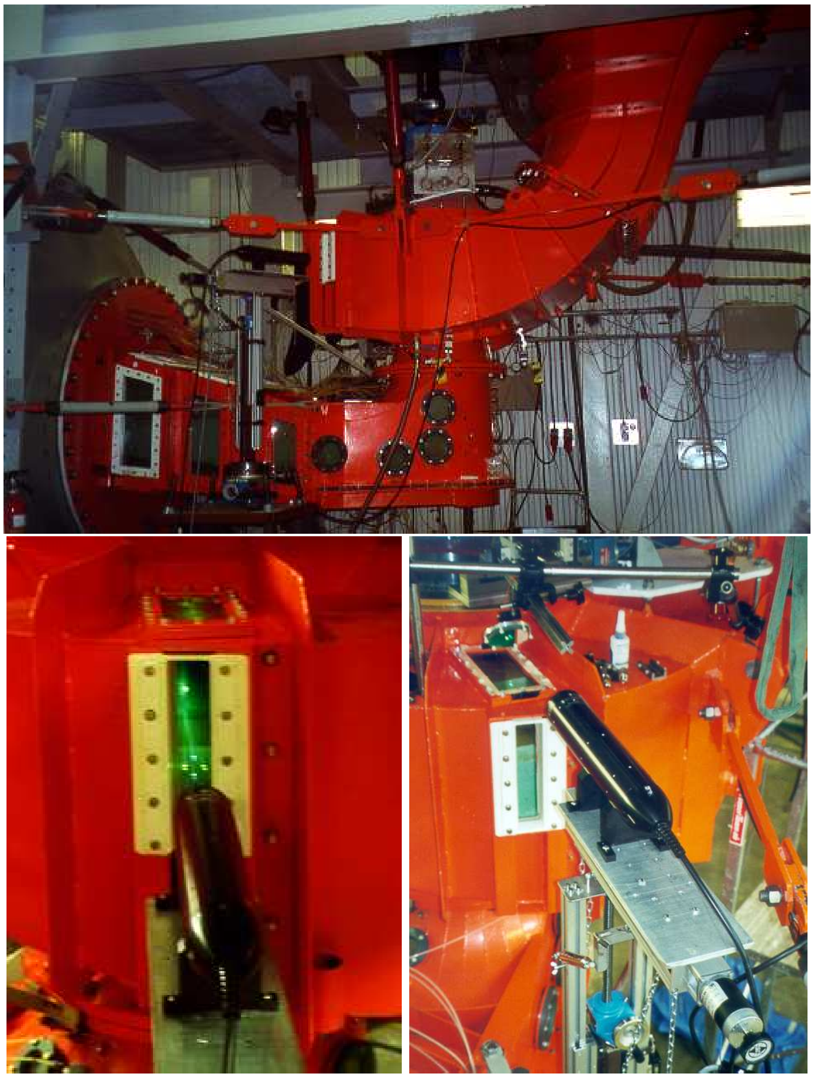

Figure 3.1: Photographs of the experimental set-up. Top and lower left: measurements 1 and 3; lower right: measurement 2.

runner blade revolutions made it possible to observe this behaviour. The measurements do not however reveal an effect large enough to be distinguished from turbulent fluctuations.

The experimental set-up and the locations of the measurements are shown in figures 3.1-3.2. The plexiglass windows allow LDV measurements of three velocity components in the spiral casing and two velocity components (tangential and axial) in the distributor. The first measurement period focused on the flow in the distributor and parts of the spiral casing (see figure 3.2(a)), where the tangential (normal to the measurement plane) and axial (vertical) velocity components were measured. These measurements were made from the window on the side of the spiral casing. The second measurement period focused on the radial velocity component at the entrance to the distributor (see figure 3.2(b)), where the tangential (normal to the measurement plane) and radial velocity components were measured. These measurements were made from the window on top of the spiral casing. The third measurement period extended the first measurement period radially outwards (see figure 3.2(c)) and measured the tangential (normal to the measurement plane) and axial (vertical) velocity components.

Restrictions on visual access and traverse equipment set the boundaries of the measurements. Unfortunately, it was necessary to make the measurements through the side of the spiral

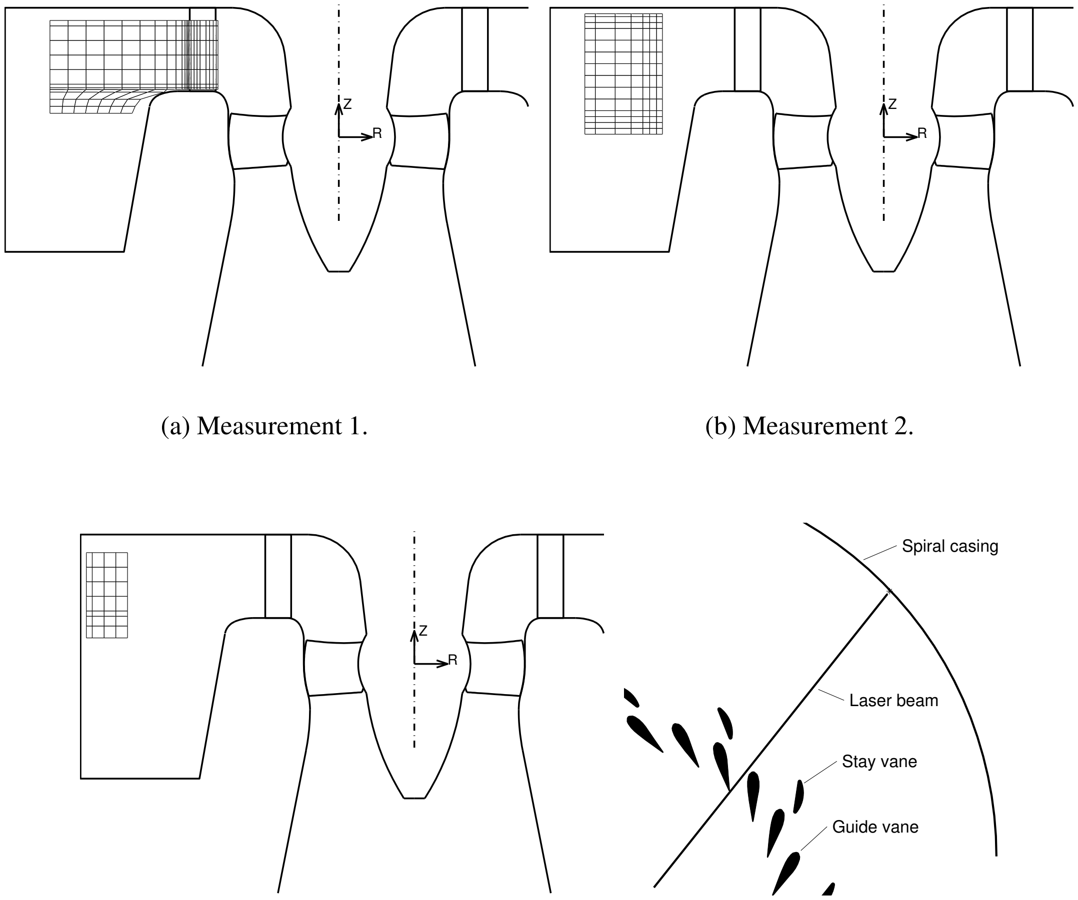

(a) Measurement 1.

(b) Measurement 2.

(c) Measurement 3.

(d) Vertical view of the direction of the measurement grid.

Figure 3.2: Schematic representation of the locations of the measurements. Measurements 1 and 3 were made through a window in the side wall of the spiral casing and measurement 2 was made through a window in the top wall of the spiral casing. The two-component LDV system thus determined the tangential and axial velocity components for measurements 1 and 3 and the tangential and radial velocity components for measurement 2.

casing slightly non-orthogonal to the plexi-glass window (10.8^o). The refraction of the laser beams was sufficient to displace the measurement volumes of the two components so that simultaneous measurement of the two velocity components was impossible. It would have been very difficult and time-consuming to calibrate this and, since the third component cannot be measured simultaneously, it was not worth the effort. The reasons for making measurements non-orthogonal to the plexi-glass window were 1) to be able to make measurements as far as possible into the distributor, 2) to avoid reflections from a guide vane (which reduces the precision and makes it impossible to make measurements close to the guide vane) and 3) restrictions on where the traversing system could be mounted. It should be noted that the measured *tangential* velocity component (normal to the measurement plane) is not exactly the true tangential velocity component, since the measurement grid had an angle of about 3 degrees from the radial direction.

4 Flow survey

The following sections present the main results of the LDV measurements and computational results of the flow in the distributor.

4.1 LDV measurements

The main results of the LDV measurements in this work are the mean velocity distribution and the RMS velocity components.

Velocity realisations have a larger likelihood to occur at higher velocities than at lower velocities. This phenomenon causes a velocity bias error. The experimental flow survey in this report is transit-time averaged to avoid velocity bias [4]. The one-time statistics (samples are treated one at a time) used in this work are

Mean	$\bar{u} = \sum_{i=0}^{N-1} \eta_i u_i$
Variance	$\sigma^2 = \sum_{i=0}^{N-1} \eta_i (u_i - \bar{u})^2$
RMS	$\sigma = \sqrt{\sigma^2}$
Turbulent intensity	$TI = \frac{\sigma}{U} \cdot 100$

where u_i is a velocity component, N is the number of samples, η_i is the velocity bias weighting factor and U is the average of each velocity component over the entire measurement region. Arithmetic averaging would bias the results in favour of the higher velocities. The bias-free method of making the statistical averages on individual realisations uses transit time weighing [4]

$$\eta_i = \frac{t_i}{\sum_{j=0}^{N-1} t_j}$$

where t_i is the transit time of the i'th particle crossing the measuring volume.

Figure 4.1 shows the results of the first measurements. The velocity normal to the measurement plane is denoted the *tangential velocity* and the vertical velocity component is denoted the *axial velocity* (positive upwards). The main features of the flow in the distributor are that the tangential velocity component increases at the lower ring (which is an effect of the sharp bend of the flow after the distributor), a stagnation region occurs in front of a guide vane, a guide vane wake region is present at the radially innermost of the measurements and there is a sharp increase in the magnitude of the axial velocity component close to the bend of the flow. The tangential turbulent intensity is largest in the wake region, close to the lower ring.

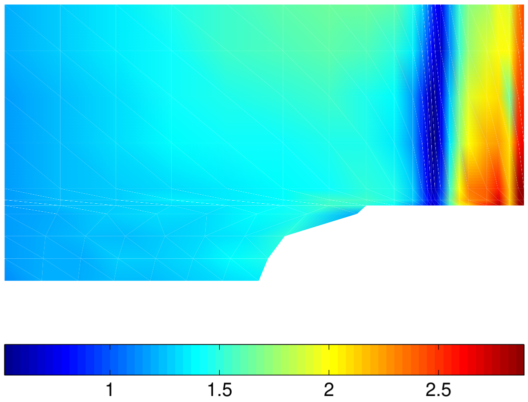

(a) Mean tangential velocity (m/s).

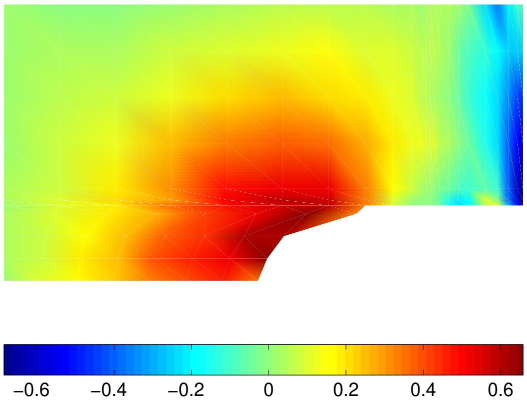

(b) Mean axial velocity (m/s).

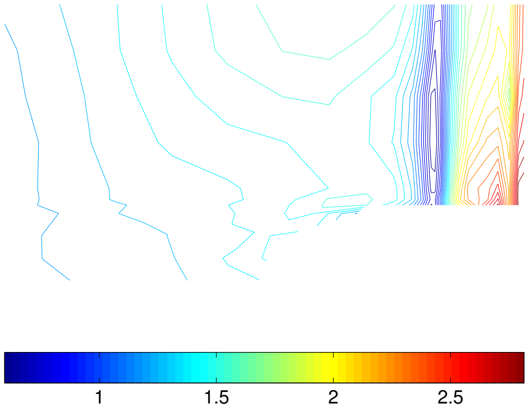

(c) Mean tangential velocity (m/s).

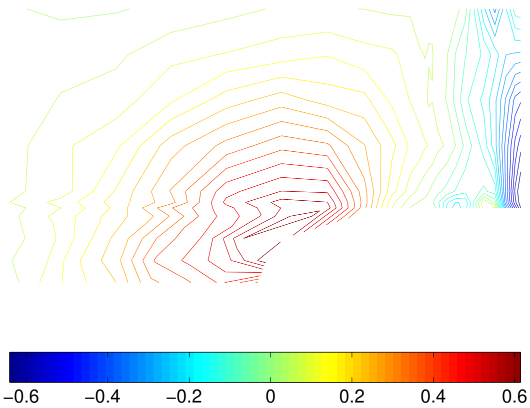

(d) Mean axial velocity (m/s).

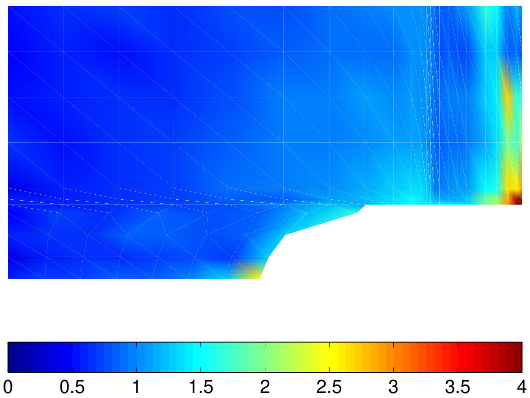

(e) Tangential turbulent intensity (%).

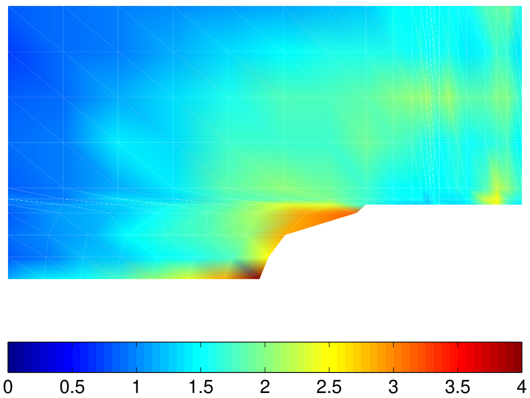

(f) Axial turbulent intensity (%).

Figure 4.1: Transit-time averaged flow survey.

Figure 4.2 shows the results of measurement 2. The velocity normal to the measurement plane is denoted the *tangential velocity*, and the velocity component along the measurement plane in the radial direction is denoted the *radial velocity*. The tangential velocity increases in the region near the entrance to the stay ring. The magnitude of the radial velocity increases towards the center line of the spiral casing and towards the upper wall of the spiral casing, which will be shown in more detail below. Both the tangential and radial turbulent intensities are greatest near the upper wall of the spiral casing.

Figure 4.3 shows the tangential and radial velocity distributions at the innermost vertical section of measurement 2 (see figure 3.2(b)). The measurements are extrapolated to the top of the spiral casing by a straight dashed line. The tangential velocity distribution is thus quite simple, with a normal boundary layer behaviour where the velocity gradually decreases to zero at the wall. However, the magnitude of the radial velocity shows a local increase close to the upper wall (note that the radial velocity is positive outwards). This behaviour might not be expected but has been observed before, both numerically and experimentally, in the flow closer to the runner [5, 7, 8]. It is thus very interesting to find the same behaviour as early as in the spiral casing.

Figure 4.4 shows the results of measurement 3. The velocity normal to the measurement plane is denoted the *tangential velocity* and the vertical velocity component is denoted the *axial velocity*. Similar to the results from measurement 2, the tangential velocity increases towards the turbine axis and towards the upper wall of the spiral casing. The axial velocity has the largest value near the outer wall of the spiral casing and towards the lower part of the measuring section. Both the tangential and axial turbulent intesities are greatest near the outer wall of the spiral casing and towards the lower part of the measuring section.

4.2 Computational results

The flow in the Hölleforsen model is being studied numerically in an ongoing project. The computations are made in two steps, first computing the flow between the guide vanes. The flow is assumed to be steady and periodic, so that it is necessary to compute only one blade passage. The result of this computation is circumferentially averaged and applied as boundary conditions in the stationary periodic runner computations [7].

Figure 4.5 shows a comparison between the results of a computation of the simplified distributor (no stay vanes and no clearance at the lower trailing edge of the guide vanes) and the measurement. The entire meridional range of the computational domain (in the same plane as the measurement grid) is shown in the figure. A black rectangle indicates where the measurement relevant for the comparison was made. The corresponding measurements are inserted in the lower left of the picture. The colors are adjusted to capture the flow features of the region in which the comparison is made. The computations thus capture the main flow features in the distributor. Some disturbances can be seen in the measurements between the guide vane stagnation region and the guide vane wake region. These disturbances most likely originate in the stay vane wake, which is not included in the computation.

5 Scientific achievements

The scientific achievements of this work are chiefly an extension of the Hölleforsen measurement data base, increased knowledge of the flow in the Hölleforsen model and the ability to validate computations in the spiral casing and the distributor of the Hölleforsen model. Com-

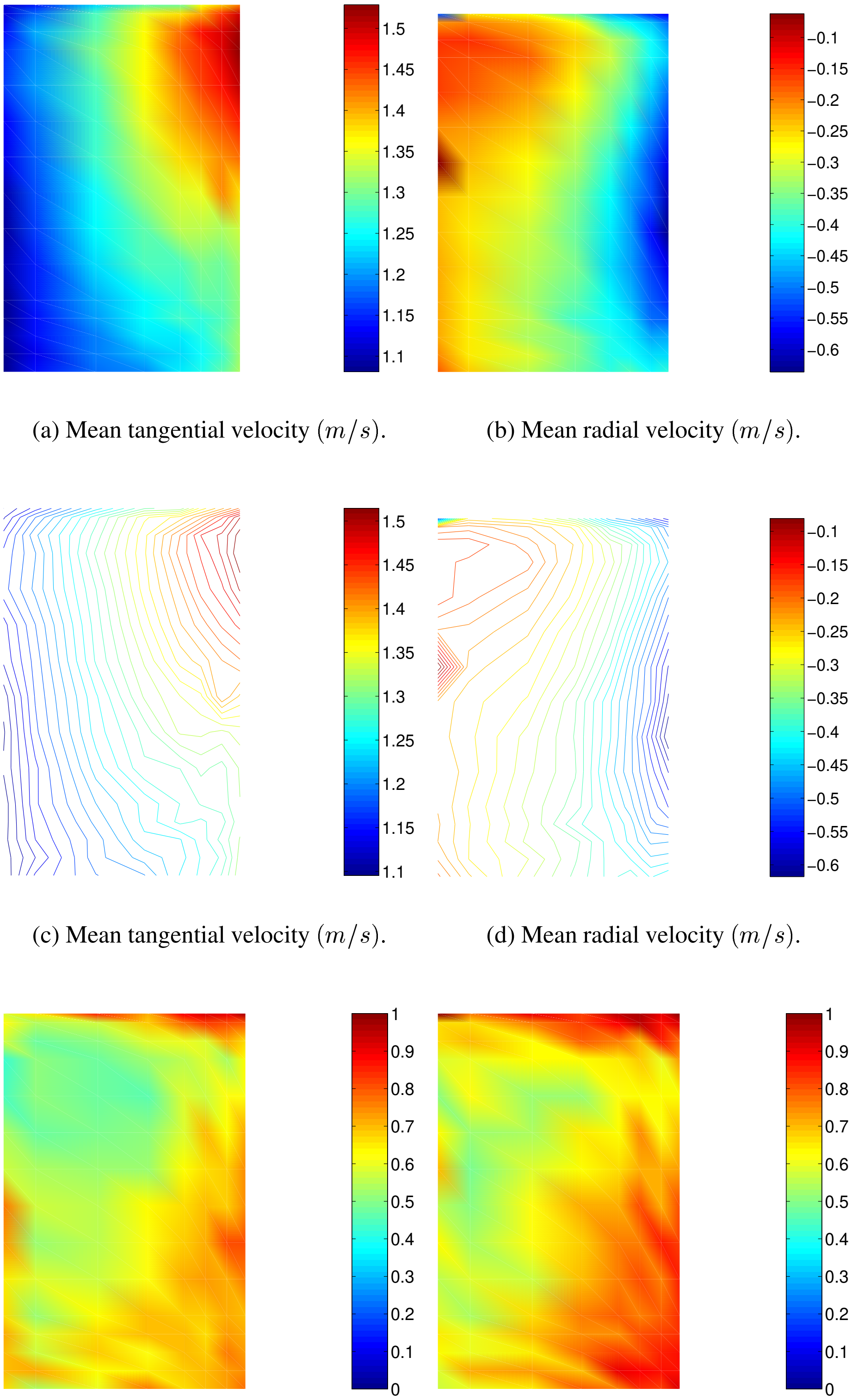

(a) Mean tangential velocity (m/s).

(b) Mean radial velocity (m/s).

(c) Mean tangential velocity (m/s).

(d) Mean radial velocity (m/s).

(e) Tangential turbulent intensity (%).

(f) Radial turbulent intensity (%).

Figure 4.2: Transit-time averaged flow survey, measurement 2.

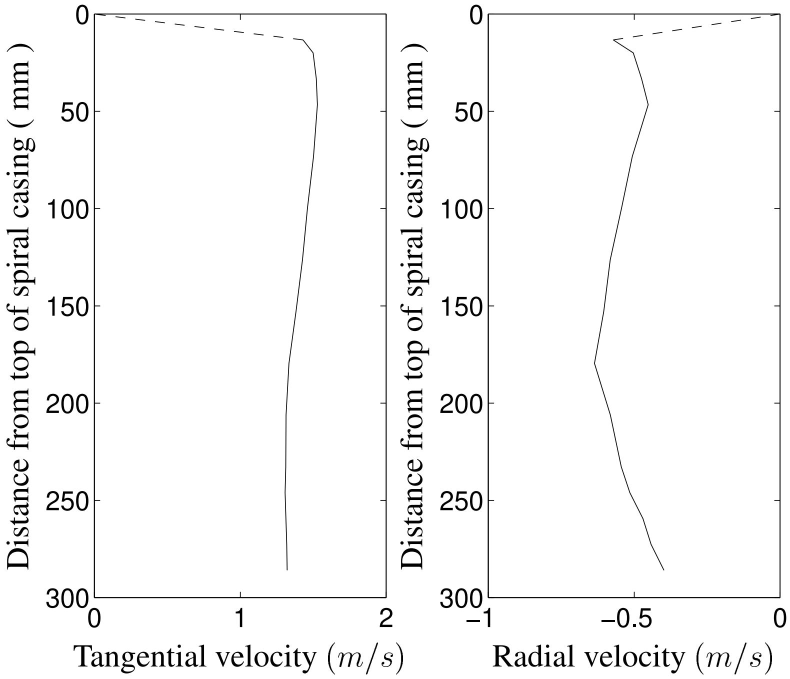

(a) Mean tangential velocity. (b) Mean radial velocity.

Figure 4.3: Transit-time averaged flow survey, measurement 2. Plot of the velocities at the innermost vertical section.

putations that are validated against the available measurements from this work and from the *Turbine 99* and the *Turbine 99 - II* workshops can be relied on for an increased knowledge of the flow in the Hölleforsen model runner.

6 Collaborative achievements

Three projects in the Swedish water turbine program and staff at Vattenfall Utveckling AB and GE Energy (Sweden) AB were involved in the measurements. Combined experience of the flow in water turbines, measurement techniques and computational techniques were discussed and shared between the collaborators. All the projects involved will gain by the results of this work: there is better knowledge of the flow in the Hölleforsen model, the results will be used in validating computations of the Hölleforsen water turbine model and measurement experience has been shared among the collaborators. The collaboration has also improved communication between the projects involved.

7 Conclusions

Quality LDV measurements were made of the flow in the spiral casing and the distributor of the Hölleforsen water turbine model. The measurements will be used for validations of computations in an ongoing project and in future computations. The computational results in the distributor show good agreement with measurements. This collaborative work has improved communication between the projects involved in the Swedish water turbine program and incre-

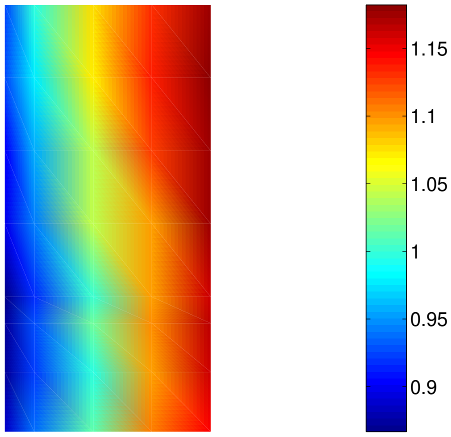

(a) Mean tangential velocity (m/s).

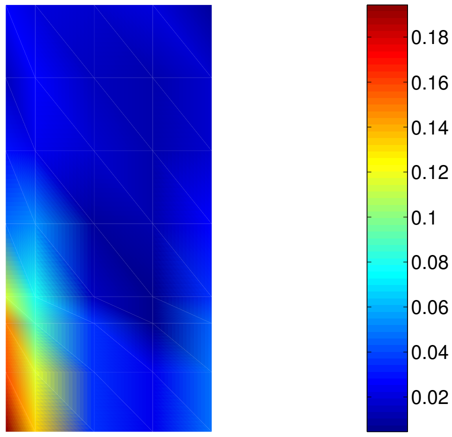

(b) Mean axial velocity (m/s).

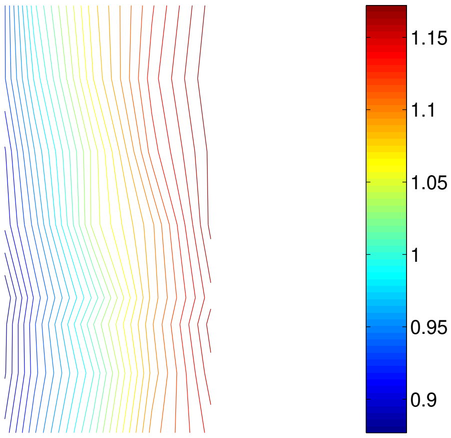

(c) Mean tangential velocity (m/s).

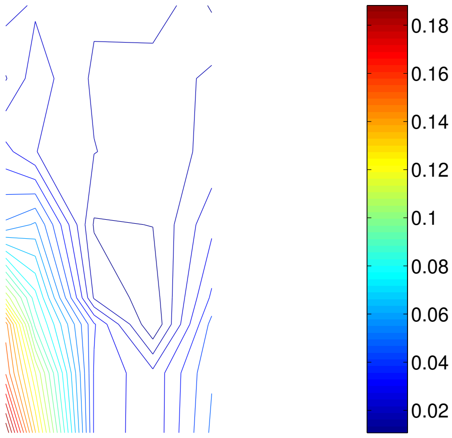

(d) Mean axial velocity (m/s).

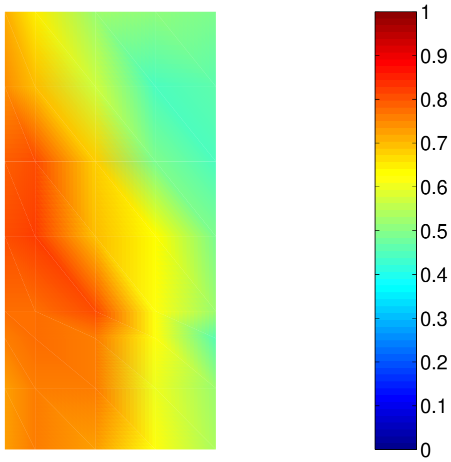

(e) Tangential turbulent intensity (%).

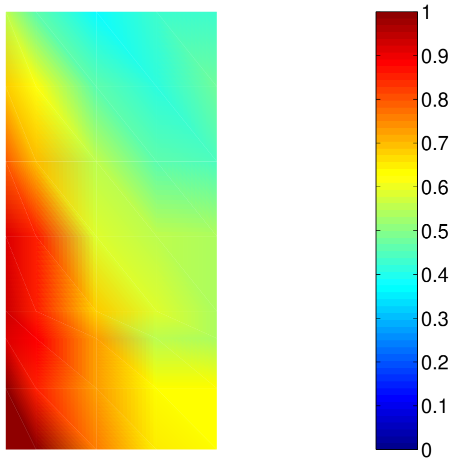

(f) Axial turbulent intensity (%).

Figure 4.4: Transit-time averaged flow survey, measurement 3.

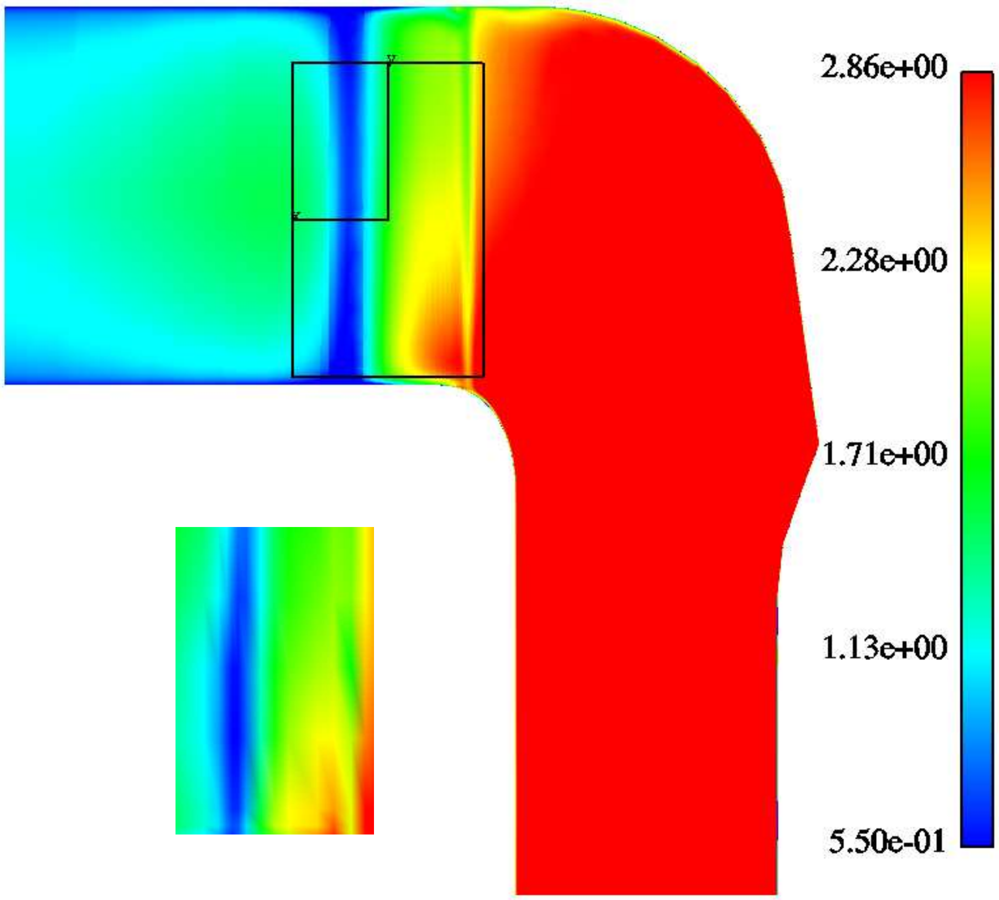

Figure 4.5: Comparison of computed and measured tangential velocity (m/s). The black rectangle indicates where the measurement relevant for the comparison was made. The corresponding measurements are inserted in the lower left of the picture. The colors are adjusted to capture the flow features of the region where the comparison is made.

ased knowledge of the flow in water turbines. Measurement experience has been gained, particularly for the projects involved whose interest is primarily of a numerical character.

References

[1] U. Andersson. An Experimental Study of the Flow in a Sharp-Heel Draft Tube. Thesis for the degree of Licentiate of Engineering 2000:08, ISSN: 1402 - 1757, Dept. of Mechanical Engineering, Division of Fluid Mechanics, Luleå University of Technology, 2000.

[2] U. Andersson. Turbine 99 - Experiments on draft tube flow (test case T). In *Proceedings from Turbine 99 - Workshop on Draft Tube Flow*, 2000, ISSN: 1402 - 1536.

[3] U. Andersson and R. Karlsson. Quality aspects of the Turbine 99 draft tube experiment. In *Proceedings from Turbine 99 - workshop on draft tube flow*, 2000, ISSN: 1402 - 1536.

[4] P. Buchhave, W.K. George, and J.L. Lumley. The measurement of turbulence with the Laser-Doppler Anemometer. *Ann. Rev. Fluid Mech.*, 11:443–503, 1979.

[5] T. Kubota. Normalization of flow profile data measured at runner inlet. In G. Sottas and I. L. Ryhming, editors, *3D-Computations of Incompressible Internal Flows - Proceedings of the GAMM Workshop at EPFL, September 1989, Lausanne - Notes on Numerical Fluid Mechanics*, pages 55–62. Vieweg, Braunschweig, 1993.

[6] J. Marchinkiewicz and L. Svensson. Modification of the spiral casing geometry in the neighbourhood of the guide vanes and its influence of the efficiency of a Kaplan turbine. In *Proceedings of the XVII IAHR Symposium, Hydraulic Machinery and Cavitation*, volume 1, pages 429–434, 1994.

[7] H. Nilsson and L. Davidson. A numerical comparison of four operating conditions in a Kaplan water turbine, focusing on tip clearance flow. In *Proceedings of the 20th IAHR Symposium, Hydraulic Machinery and Cavitation*, 2000.

[8] H. Nilsson and L. Davidson. A validation of parallel multiblock CFD against the GAMM Francis water turbine runner at best efficiency and off-design operating conditions. Int.rep. 01/02, Dept. of Thermo and Fluid Dynamics, Chalmers University of Technology, Gothenburg, 2001.

Acknowledgements

This work is financed and supported by ELFORSK (Swedish Electrical Utilities Research and Development Company), the Swedish National Energy Administration and GE Energy (Sweden) AB.

Vattenfall Utveckling AB and its staff are gratefully acknowledged for their contribution of equipment and knowledge.